Label-Free Noninvasive Cell Characterization

James C.M. Hwang

As an electrical engineer, I like to view everything, large or small, in terms of an equivalent circuit of resistors, capacitors, inductors, and other components. To help me understand cell biology, I attempted to put together a simple equivalent circuit for a cell and validate it by electrical measurements. I soon found sympathy with far-sighted physical scientists and engineers from a century ago whose knowledge of biology was as poor as mine is now—not because they were too lazy to learn but because, back then, the knowledge did not exist. They made me sweat because, despite

James C.M. Hwang (jch263@cornell.edu) is with the Department of Materials Science and Engineering, Cornell University, Ithaca, New York, 14853, USA.

Digital Object Identifier 10.1109/MMM.2021.3056834
Date of current version: 2 April 2021

working with a suspension (mixture) of millions of cells, they gained insight into a single cell with the help of Maxwell [1] and Wagner [2].

Is a Cell a Bunch of Resistors and Capacitors?

In 1902, Bernstein hypothesized [3] that a cell is made of a membrane wrapping around a cytoplasm of electrolytes. The hypothesis can be represented by the equivalent circuit in Figure 1(a) [4]. Here, the membrane is represented by a parallel circuit of resistance R_M and capacitance C_M,, and the cytoplasm is represented by another parallel circuit of R_C and C_C. We do not need an inductor because the membrane is thin and the cytoplasm is fat in cross section. Normally, we need to keep a cell alive in a saline solution. However, if we press sharp electrodes next to the cell so that most of the electric field goes through it, neither do we need to include the solution in the equivalent circuit [5]. Now, if we know the approximate values of R_M, C_M, R_C, and C_C, we can have some idea about the impedance spectrum of a cell.

The Bernstein cell model was experimentally validated first by Höber, in 1910 [6], [7]. Höber not only proved that a cell contains free-moving electrolytes but also estimated the cytoplasm resistivity to be on the order of 1 MΩ. (His estimate remains valid today [8].) Because I am kind of square, I further simplify the cell from a sphere to a cube of 10 μm on each side [9]. In this case, $R_C \approx 0.1$ MΩ. Because living things are mostly water, we can approximate the cytoplasm permittivity with that of water. Therefore, $C_C \approx 10$ fF. In 1921, Philippson [10] measured the membrane resistance of a cubic centimeter of guinea pig liver to be about 2 kΩ. Scaling it to a cube of 10 μm on each side and considering that there are two membranes (top and bottom), $R_M \approx 1$ MΩ. In 1925, Fricke [11] measured the membrane capacitance of a suspension of dog blood cells to be on the order of 1 μF/cm^2. Therefore, $C_M \approx 1$ pF.

I soon found sympathy with far-sighted physical scientists and engineers from a century ago whose knowledge of biology was as poor as mine is now.

With $R_M \approx 1$ MΩ, $C_M \approx 1$ pF, $R_C \approx 0.1$ MΩ, and $C_C \approx 10$ fF, we can simulate the impedance (admittance) spectrum of a cell, as shown in Figure 1(b) [12]. We can see that the conductance of the cell as a whole is dominated by R_M in the kilohertz range and by R_C in the megahertz range. Similarly, the cell capacitance is dominated by C_M in the megahertz range and by C_C in the gigahertz range. Also, we can use the plateaus in Figure 1(b) to separately extract R_M, C_M, R_C, and C_C if we measure the cell impedance in the right frequency ranges. However, electrical engineers are used to a system impedance of 50 Ω and have a hard time dealing with a resistance as large as 1 MΩ or a capacitance as small as 10 fF. Luckily, we need to measure 10 fF only in the gigahertz range, which is at least easier than what the pioneers tried to do in the kilohertz and megahertz ranges because the admittance of a capacitor rises with increasing frequency.

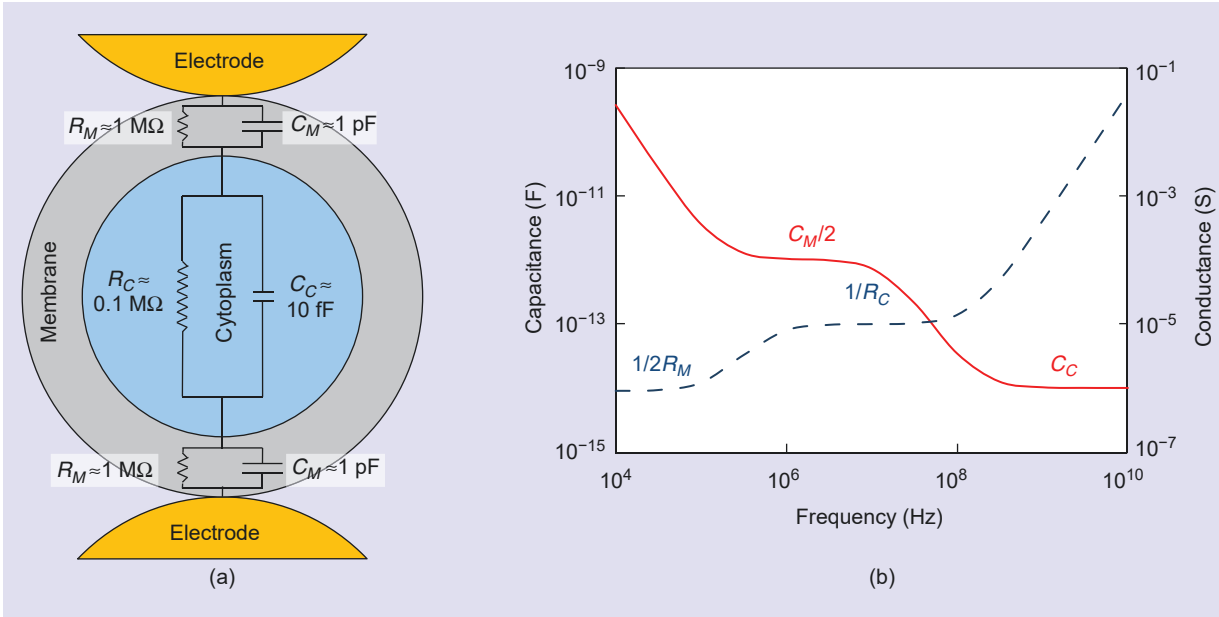

Figure 1. *The (a) equivalent circuit of a cell and (b) the cell's simulated admittance spectrum [12].*

Cole and His Equation

Cole was another pioneer in the impedance spectroscopy of cells and other materials a century ago. The Cole–Cole equation [S1] is a dielectric relaxation model,

$$\varepsilon^*(\omega) = \varepsilon_\infty + \frac{\varepsilon_S - \varepsilon_\infty}{1 + (j\omega\tau)^{1-\alpha}}, \tag{S1}$$

where ε^* is the complex permittivity, ε_S and ε_∞ are the static and infinite-frequency dielectric constants, ω is the angular frequency, τ is a time constant, and $0 < \alpha < 1$. The exponent α describes different spectral shapes. When $\alpha = 0$, (S1) reduces to the Debye equation [S2]:

$$\varepsilon^*(\omega) = \varepsilon_\infty + \frac{\varepsilon_S - \varepsilon_\infty}{1 + j\omega\tau}. \tag{S2}$$

When $\alpha > 0$, the relaxation is stretched across a wider range of ω than the Debye equation. For multiple relaxation mechanisms with time constants $\tau_1, \tau_2, \ldots \tau_N$, (S2) can be expanded into a series as [S3]

$$\varepsilon^*(\omega) = \varepsilon_\infty + \frac{\varepsilon_S - \varepsilon_2}{1 + j\omega\tau_1} + \frac{\varepsilon_2 - \varepsilon_3}{1 + j\omega\tau_2} \cdots \frac{\varepsilon_N - \varepsilon_\infty}{1 + j\omega\tau_N}. \tag{S3}$$

If necessary, (S1) can be similarly expanded.

References

[S1] K. S. Cole and R. H. Cole, "Dispersion and absorption in dielectrics: I—Alternating current characteristics," *J. Chem. Phys.*, vol. 9, no. 4, pp. 341–351, 1941. doi: 10.1063/1.1750906.

[S2] P. Debye, "Zur theorie der anomalen dispersion im gebiete der langwelligen elektrischen strahlung," *Ber. Dtsch. Phys. Ges.*, vol. 15, no. 16, pp. 777–793, 1913.

[S3] T. Kotnik and D. Miklavcic, "Theoretical evaluation of distributed power dissipation in biological cells exposed to electric fields," *Bioelectromagnetics*, vol. 21, no. 5, pp. 385–394, July 2000. doi: 10.1002/1521-186X(200007)21:5<385::AID-BEM7>3.0.CO;2-F.

According to Foster [13], "By the early 1940s, the large dispersion in cell suspensions centered near 1 MHz (which became known in Schwan's terminology as the β dispersion) had been known by Cole and others to arise from charging of the membrane capacitance" (see "Cole and His Equation"). Obviously, Höber, Philippson, and Fricke knew this, so, not long after the spark gap transmitter was developed [14] by Hertz to prove the existence of the radio wave predicted by Maxwell, they used the spark gap to extend the measurements higher than 1 MHz. Notice that Philippson pioneered radio broadcasting in Belgium [7], Fricke studied atomic physics in Denmark under Bohr and became an authority in radiobiology [15], and Schwan supported his graduate study by working as a radio technician for Telefunken and

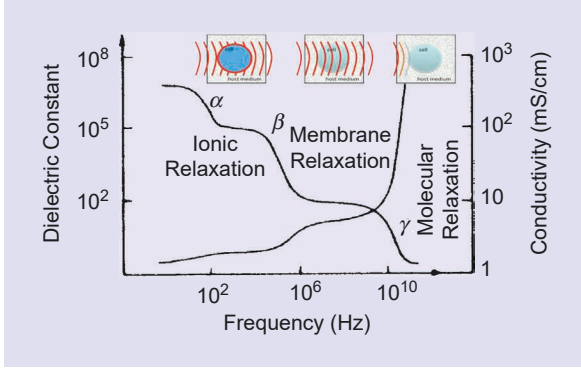

Figure 2. *Schwan's hypothesized cell relaxation mechanisms [17] and the corresponding penetration depths of the microwave signal illustrated by Grenier's group [18].*

was known as the father of bioengineering [13]. These physical scientists and engineers helped to pioneer modern biology.

An Alphabet Soup

In addition to the β dispersion around 1 MHz, Schwan [16] found dispersions in the kilohertz and gigahertz impedance spectra of tissues and cell suspensions, which he named α and γ dispersions, respectively, as noted in Figure 2 [17]. You can see that Figures 1(b) and 2 are very similar, confirming that a simple equivalent circuit of frequency-independent resistances and capacitances can simulate the complicated dispersion of a cell. In essence, we simulate the different dispersions by various R and C time constants—an old trick of electrical engineers. However, an equivalent circuit does not equal the real thing. It is not unique because many different circuit topologies can simulate the same behavior. As a minimalist, I like this equivalent circuit for its simplicity. At least, it is a convenient way to summarize the measured impedance spectrum of a cell, making it easier to compare the results from experiment to experiment, group to group, and century to century.

Schwan was careful to call the ionic, membrane, and molecular relaxation mechanisms of Figure 2 *hypotheses*. He was also careful to use the term *relaxation* or *dispersion* and never *resonance*. Those who like to associate a spectrum with sharp resonance lines will be disappointed. Unlike atoms, molecules, and crystals, the heterogeneous structure of a cell naturally leads to broad dispersions typical of all

living things. (For example, I am not very sharp.) A corollary is that resonance detectors may not be very useful here. We have plenty of sensitivity once we replace a one-port impedance measurement with a two-port scattering (*S*) parameter measurement. At issue is the signal-to-noise ratio, not the sensitivity. To get to know a cell well, we need to do broadband spectroscopy across many decades of frequency. For this, electrical engineers have a network analyzer that coherently covers many decades of frequency. In comparison, an optical engineer has to spend a fortune to buy a laser that is tunable for only a small section of the spectrum.

On top of Schwan's hand-drawn impedance spectrum, I took the liberty to copy and paste computer-generated graphs from Grenier's group [18]. These illustrate very well the need for broadband spectroscopy. This is because, in the kilohertz range, microwaves cannot penetrate the cell membrane but are sensitive to the overall size and shape of a cell. In the megahertz range, microwaves can bypass the membrane capacitance to nondestructively sense inside a cell. Near the terahertz range, microwaves again cannot penetrate very far but can sense what is on the cell membrane (hopefully not a virus). Therefore, we can use microwaves of different frequencies to learn the multiple personalities of a cell. Here, I use the broad definition of *microwave* to mean from RF to terahertz frequencies.

I learned a lot not only from the pioneers a century ago but from contemporaries, such as Grenier. However, unlike many contemporaries, I like to say "impedance spectroscopy" instead of "dielectric spectroscopy." What's in a name? As mentioned previously, it is easier to compare the impedance spectrum from one group to another. Dielectric electrical (oxymoron) engineers like to report dielectric constants and conductivities. Theoretically, instead of resistances and capacitances, a cell can also be represented by dielectric constants and conductivities. However, to a real electrical engineer, resistances and capacitances are directly measurable, but dielectric constants and conductivities are inferred after assumptions of cell size, cell shape, and membrane thickness. The membrane thickness was first determined by Fricke as 3 nm [11] and confirmed by d'Inzeo's group almost a century later [19]. (Living things are fluid. It does not count if you dry a cell before you check it under an electron microscope.) Yet many researchers neglect the membrane thickness in reporting a dielectric spectrum. Also, for a biological ignorant like me, I see in Figure 2 three cliffs and three plateaus in the capacitance spectrum and six similar features in the conductance spectrum. I will have a hard time trying to decide a cell model with more than 12 parameters, especially if I can't measure a cell across many decades of frequency. I will be totally lost if I have to define each permittivity in a frequency-dependent series, such as (S3), even though I greatly admire Cole and Debye.

Electrical engineers are used to a system impedance of 50 Ω and have a hard time dealing with a resistance as large as 1 MΩ or a capacitance as small as 10 fF.

Microwaving a Cell Alive

Almost every day, I microwave about a trillion cells for lunch, because my stomach is roughly 1,000 cm^3 and a cell is approximately 1,000 μm^3. However, I have a hard time aiming the microwave at just one cell. To do that, I have to overcome not only the impedance mismatch but the size mismatch. A network analyzer is about the size of a microwave oven, which means it is more than a trillion times bigger than a cell. Above all, I must keep the cell happy so that it shows its true colors. For these reasons, my group uses several tricks [9]:

1) Resuspend cells in an isotonic sucrose solution to minimize the solution effects while keeping cells alive. (Many of us are sugar freaks, too.)
2) Use ac dielectrophoresis (see "Dielectrophoresis") [20] to quickly trap and release a cell between closely spaced electrodes and to focus the electric field inside the cell.
3) Replace a one-port impedance measurement with a two-port *S*-parameter measurement to increase the dynamic range.
4) Use rapidly successive measurements with and without a cell to perform an interference measurement in the time domain instead of the spatial domain. (It is difficult to null an interferometer in the spatial domain through decades of frequency and for longer than a few minutes.)
5) Use the same ultrawideband network analyzer to quickly switch between trapping, characterization, electroporation [21], and release (Table 1).

We follow Höber [6] to resuspend cells in a sucrose solution that is much less conductive than the medium for cell cultures [22]. This helps to minimize side effects, such as electrolysis and electrode polarization [23]. However, although the solution is isotonic and cells remain alive and spherical for many hours [9], the cells' diameter and cytoplasm conductivity may decrease slightly. (In general, there are many subtle

An equivalent circuit does not equal the real thing. It is not unique because many different circuit topologies can simulate the same behavior.

issues in relating in vitro measurements to in vivo behaviors, which are beyond the scope of this article.) Presently, at least when live and dead [24] cells are suspended in sucrose, there is no significant difference in their size distributions, as demonstrated in Figure 3. We can see in the figure wide distributions in the cell diameter, reflecting biological heterogeneity. However, live and dead cells appear to have the same average diameters. Note that, in this case, the dead cells are gently killed by heating them to 60 °C, a process similar to pasteurizing food without spoiling its taste.

Because the network analyzer is much more sensitive than an impedance meter, we can use an input power as low as –18 dB below 1 mW to obtain the impedance spectrum of a cell (Table 1). This power level is orders of magnitude lower than that required for reversible electroporation [21], let alone heating and otherwise hurting the cell. (It is not worthwhile to microwave just one cell for lunch.) We do not know how happy a cell is about being trapped. However, we have trapped and interrogated a cell for more than an hour, and its impedance does not fluctuate beyond the background noise. By contrast, the difference in the impedance of live and dead cells (0.01 dB) is about an order of magnitude larger than the background noise of the measurement setup (0.001 dB) [24]. Right now, the calibration of the experimental setup drifts by about 0.01 dB per hour [12]. If the stability of the setup is improved, it will be interesting to use it to track a cell's impedance as it gets tired or old.

We tried these tricks on Jurkat cells [25]. Jurkat is a well-studied cloning line of human T-lymphocyte cells with a spherical shape, large diameter (~10 μm), and simple structure. The cells do not stick around to clog up a microfluidic channel and can be flown through one by one and trapped on a coplanar waveguide (CPW), as illustrated in Figure 4. We taper the CPW precisely down to a 10-μm trap in a series or shunt configuration (Figure 5) while maintaining a 50-Ω characteristic impedance through many decades of frequency. Figure 6 displays the measurement setup with the CPW placed on a homemade probe station, which is, in turn, on an inverted fluorescence microscope for simultaneous electrical and optical characterization [21]. Simultaneous optical characterization

Dielectrophoresis

Dielectrophoresis (DEP) has been used by biologists for decades not only in cell manipulation but in sorting and characterization through a cytometer [S4]. Recently, the groups of Bridges [S5] and Pothier [S6] advanced DEP higher than 100 MHz, making it more sensitive to R_C. However, because DEP is based on fluid dynamics, the technique is sensitive to the cell size and shape at most frequencies. Bridges' group overcomes the challenge by focusing at 6 MHz, where the dependence on cell diameter changes sign and is at a minimum.

References

[S4] R. Pethig, *Dielectrophoresis: Theory, Methodology and Biological Applications*. Hoboken, NJ: Wiley, 2017.

[S5] S. Afshar et al., "Full beta-dispersion region dielectric spectra and dielectric models of viable and non-viable CHO cells," *IEEE J. Electromagn. RF Microw. Med. Biol.*, early access, 2020. doi: 10.1109/JERM.2020.3014062.

[S6] T. Provent et al., "A high frequency dielectrophoresis cytometer for continuous flow biological cells refinement," in *Proc. Eur. Microw. Conf. (EuMC)*, Jaarbeurs Utrecht, The Netherlands, Jan. 2021, pp. 921–924.

TABLE 1. A network analyzer's frequency and power.

Function	Frequency	Power
Trapping	10 MHz	0 dBm
Characterization	9 kHz–9 GHz	–18 dBm
Electroporation	100 kHz	9 dBm
Release	10 kHz	3 dBm

dBm: decibel referenced to 1 mW.

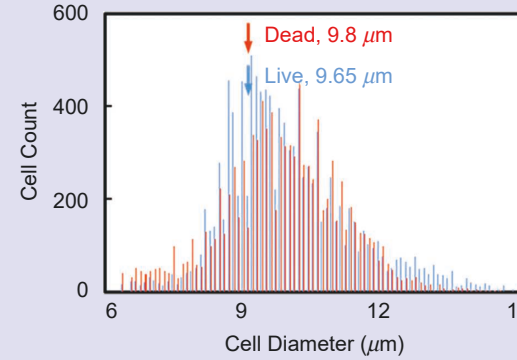

Figure 3. *The size distribution of live and dead Jurkat cells resuspended in an isotonic sucrose solution and analyzed by a Coulter counter.*

is critical to many biologists for whom "seeing is believing."

Figure 7 compares the measured and simulated S parameters of the CPW with a series or shunt trap and the microfluidic channel filled with air or sucrose. We can see that the measurement setup takes full advantage of the 100-dB-plus dynamic range of a two-port measurement, and the CPW behaves smoothly across many decades of frequency. Because the impedance of a cell is on the order of 1 MΩ, Figure 7 shows that, with a series trap, the reflection coefficient $S_{11} \approx 1$ (0 dB), while the transmission coefficient $S_{21} \approx 0$ ($-\infty$ dB). On the other hand, with a shunt trap, $S_{11} \approx 0$, while $S_{21} \approx 1$. We see in the next section that, despite being very small, S_{21} is more sensitive to a series-trapped cell, while S_{11} is more sensitive to a shunt-trapped cell. This is counterintuitive but agrees with the

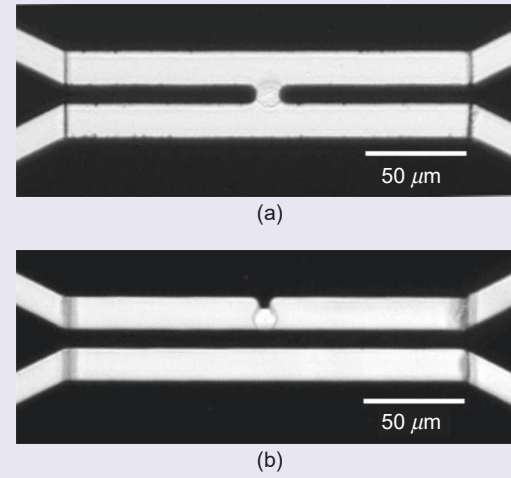

Figure 5. *A Jurkat cell trapped by dielectrophoresis on a CPW in (a) a series and (b) a shunt configuration [12].*

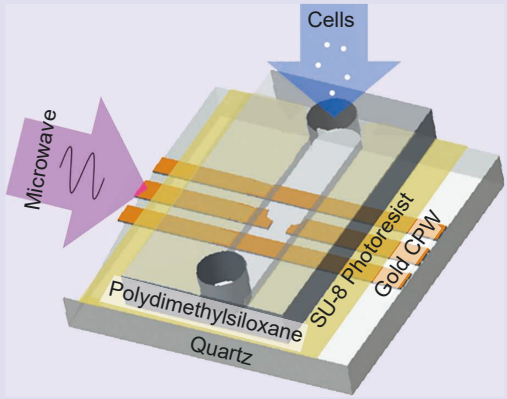

Figure 4. *Cells delivered via a microfluidic channel to be trapped on a CPW for impedance spectroscopy [12].*

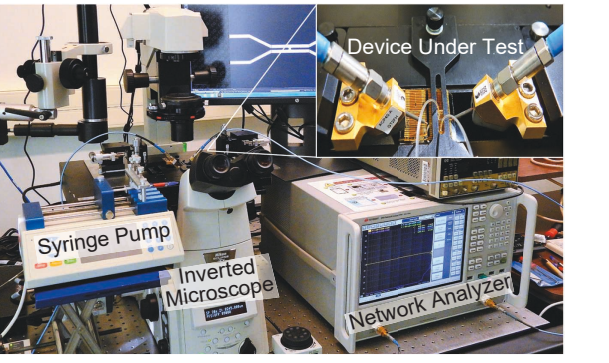

Figure 6. *The measurement setup with the CPW on a homemade probe station on top of an inverted fluorescence microscope [12].*

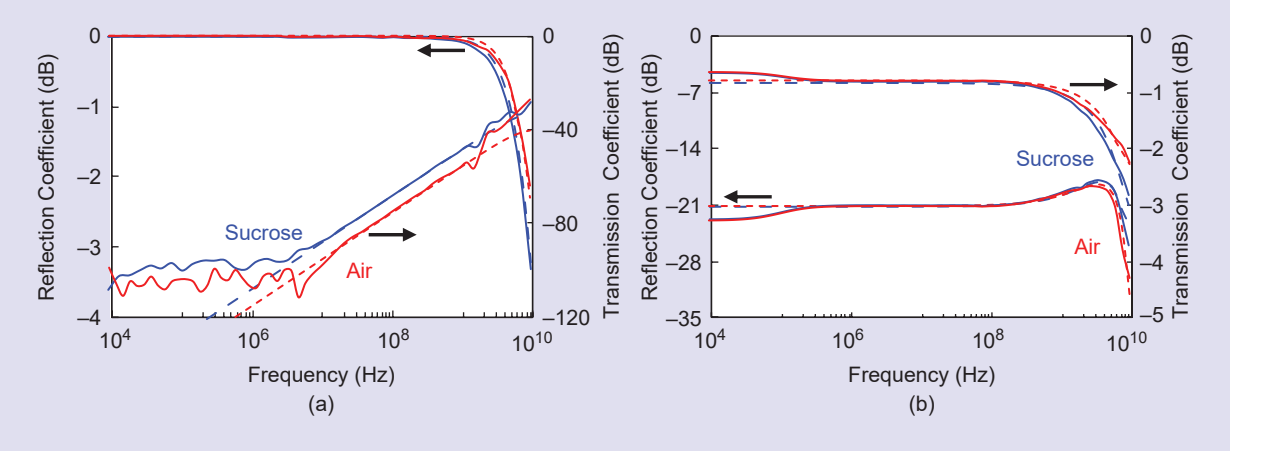

Figure 7. *The measured (solid) versus simulated (dashed) magnitudes of the reflection and transmission coefficients of a CPW with (a) a series or (b) a shunt trap filled with air or sucrose solution [12].*

Broadband impedance spectroscopy is a convenient way to quickly tell whether a cell is alive or dead, without dyeing and culturing.

sensitivity analysis [12]. It also underscores the complementary nature of the series and shunt traps as well as the importance of the two-port measurement and dynamic range.

Impedance of a Jurkat Cell

On the scales in Figure 7, we cannot see any difference in S_{11} and S_{21} with or without a cell trapped. We can see the difference only when it is plotted by itself, as in Figures 8 and 9. Here, the reflection change $\Delta|S_{11}|$ and transmission change $\Delta|S_{21}|$ are defined, in decibels, as

$$\Delta|S_{11}| = 10\cdot\log\left|S_{11}^{\text{w/cell}}\right| - 10\cdot\log\left|S_{11}^{\text{w/o cell}}\right|, \quad (1)$$

$$\Delta|S_{21}| = 10\cdot\log\left|S_{21}^{\text{w/cell}}\right| - 10\cdot\log\left|S_{21}^{\text{w/o cell}}\right|. \quad (2)$$

We repeated the measurement many times, each with a different cell trapped in a series or a shunt configuration. We plot their average values along with error bars. Comparing the measured $\Delta|S_{11}|$ and $\Delta|S_{21}|$ with those simulated using different combinations of R_M and C_C, we can determine their values to the second digit despite weak and noisy data. Table 2 summarizes the R_M and C_C values that

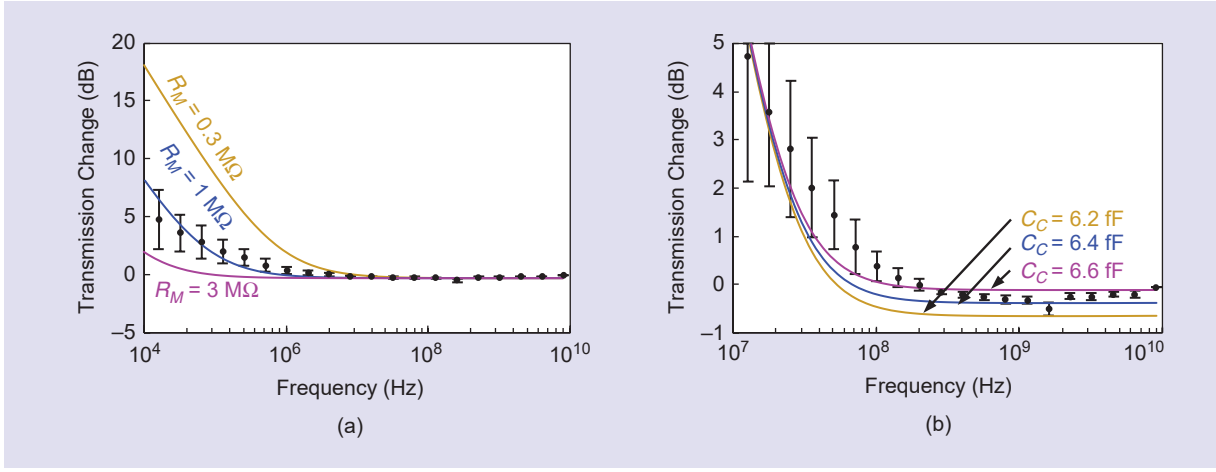

Figure 8. *The measured (symbols) versus simulated (curves) changes in the transmission coefficient for a CPW with a live Jurkat cell trapped in the series configuration. The simulations are performed with (a) R_M = 0.3, 1, and 3 MΩ; C_C = 6.4 fF and (b) R_M = 1.5 MΩ; C_C = 6.2, 6.4, and 6.6 fF. In all cases, C_M = 0.3 pF, and R_C = 0.4 MΩ [12].*

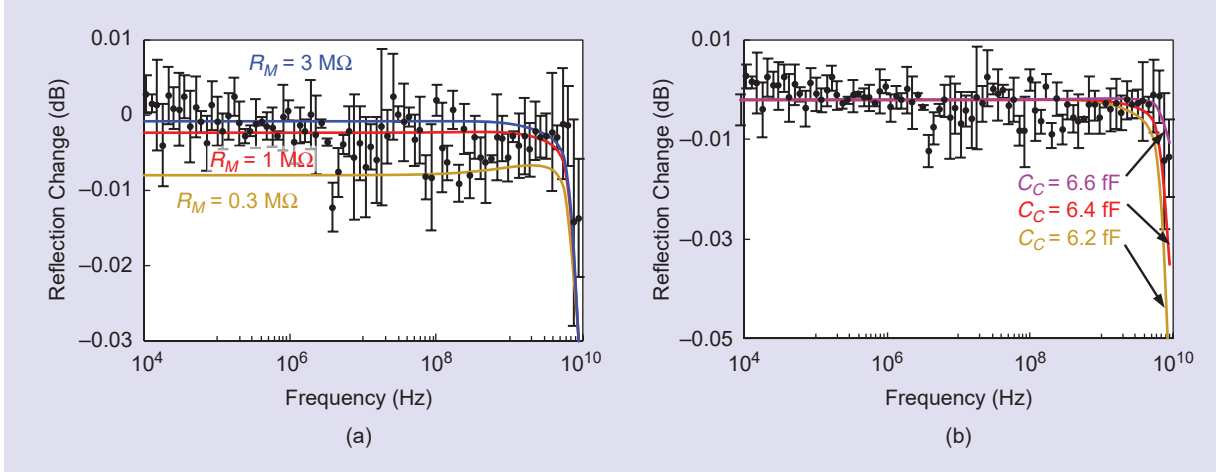

Figure 9. *The measured (symbols) versus simulated (curves) changes in the reflection coefficient for a CPW with a live Jurkat cell trapped in the shunt configuration. The simulations are performed with (a) R_M = 0.3, 1, and 3 MΩ; C_C = 6.4 fF and (b) R_M = 1.5 MΩ; C_C = 6.2, 6.4, and 6.6 fF. In all cases, C_M = 0.3 pF, and R_C = 0.4 MΩ [12].*

TABLE 2. The electrical characteristics of a Jurkat cell.

R_M (MΩ)	C_M (pF)	R_C (MΩ)	C_C (fF)	Bandwidth (MHz)	Reference
–	1.1	0.13	6	0.01–100	[26]
3.6	1.4	0.15	6	0.01–100	[27]
80	1.1	0.2	12	0.01–100	[28]
20	0.9	0.5	–	Nanosecond pulse	[29]
2	1.2	0.3	6	0.01–10	[30]
–	0.7	0.2	10	0.001–100	[31]
1.5 ± 0.3	1.5 ± 0.3	0.4 ± 0.1	6.4 ± 0.1	0.009–9,000	This work

give the best fit, together with a similarly fitted R_C and C_M. For comparison, Table 2 includes values found in the literature, mostly measured on cell suspensions in the kilohertz-to-megahertz range, with single-cell characteristics in terms of dielectric constants and conductivities extracted using the Maxwell–Wagner mixture model [1], [2]. To make the comparison easier, I have converted the literature values into resistances and capacitances using my simple cubic-cell model because many researchers do not report the shape of the cell. In cases where they do not report either the cell size or membrane thickness, I use 10 μm and 10 nm, respectively.

It hurts my ego to see from Table 2 that, after working so hard to measure a single cell across a broad bandwidth, our results are not much different from those of others except for being more precise. Besides making everyone happy by validating the Maxwell–Wagner mixture model, why do we need to measure C_C within ±0.1 fF? Well, 0.2 fF may mean the difference between life and death [24]. However, it is difficult to precisely measure C_C below 100 MHz, as illustrated in Figure 1(b). Since other measurements are all less than 100 MHz [26]–[31], I suspect that, instead of directly measuring C_C, they estimate C_C by assuming that the dielectric property of the cytoplasm is similar to that of a saline solution, just as I did in the "Is a Cell a Bunch of Resistors and Capacitors?" section for an order-of-magnitude estimate of C_C.

Broadband impedance spectroscopy is a convenient way to quickly tell whether a cell is alive or dead, without dyeing and culturing [24]. As impedance spectroscopy advanced from the kilohertz to the gigahertz range, cell characterization also advanced from R_M to C_M and R_C, starting from Philippson's discovery that the R_M of a guinea pig's muscle cells decreases after the animal dies [10]. With the most recent advancement to C_C, we can more thoroughly and reliably characterize the physiological state of a cell. For example, we found that, as a Jurkat cell dies, C_M decreases, but R_C and C_C increase [24]. Because of biological heterogeneity, multimodal measurement is necessary to minimize false alarms. It is too risky to sort cells based on just one parameter, whether it is R_M, C_M, R_C, or C_C.

What Is Next?

A cell is actually more complicated than I can comprehend. So far, we assume a homogenous cytoplasm inside a cell. However, a cell often contains a nucleus and many other kinds of organelle. As we continue to improve the measurement technique, we can use a more complicated equivalent circuit to extract additional subtleties from a cell. Figure 10 conveys the equivalent circuit for a double-shell cell [32], [33]. In this model, we have added R_N and C_N to account for the nuclear plasma and R_{NM} and C_{NM} for the nuclear membrane. Here, R_{C1} and C_{NM1} account for the signals bypassing the nuclear membrane and plasma, respectively. For the sake of completeness, R_{EXT}, C_{EXT}, and C_{BIAS} account for the solution effects. Altogether, there

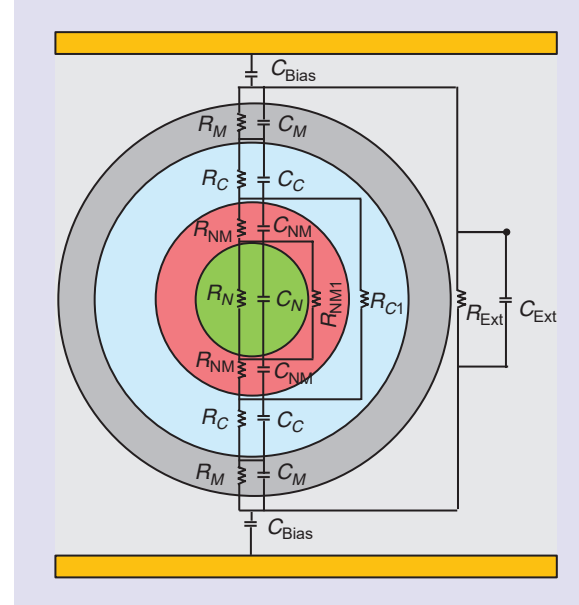

Figure 10. *The equivalent circuit of a double-shell cell.*

If we can show the promise of the technique, clever people will figure out ways to drastically improve its throughput and make a fortune from commercializing it.

are 13 parameters—one too many. However, we may be able to extract the parameter from the exact shape of the β dispersion, as in (S1). Recently, we have been able to tell from the impedance spectrum the nuclear size of a live cell [34] by expanding the bandwidth to between 900 Hz and 40 GHz. To further expand the bandwidth, the CPW needs to be more linear, the signal-to-noise ratio needs to be higher, and the network analyzer needs to be cheaper.

I thought life would be simpler dealing with only one cell at a time. Once we start to peer inside the cell, I realize I have traded a suspension of cloned cells for a suspension of different organelles. Since Maxwell and Wagner are no longer available, I look elsewhere for help. What Maxwell and Wagner did not have is a computer running a 3D, finite-element, full-wave electromagnetic simulator. We have successfully used it with help from Liberti's group [5]. However, many challenges remain because the electric field distribution is highly

1) nonuniform, giving a cell size comparable to the electrode size and gap
2) perturbed by the presence of the cell
3) dispersive with the heterogeneous structure of the cell
4) asymmetrical, because the cell may be skewed and does not sit still
5) multiscale, from a centimeter-long CPW to submicron organelles.

To improve the measurement precision, we need to better the calibration technique. For the characterization of nanoliter liquids, we have collaborated with Booth's group to develop a single-connection in situ calibration technique using liquids of known permittivity [35]. Recently, we have applied single-connection calibration to move the reference plane from the probe tip to the edge of the microfluidic channel for distinguishing cells with different nuclear sizes [22]. The calibration technique should make it easier to adapt broadband electrical characterization to a cytometer, following Niknejad's group [36].

A cell may appear homogeneous again if the electrode is much smaller than the cell. For this, we have developed with Farina's group a broadband, quantitative, and biocompatible scanning microwave microscope from an atomic force microscope [37], [38]. We can use it not only to resolve subcellular structures but also to study bacteria and viruses that are much smaller than 10 μm [39]. Alternatively, we can improve the spatial resolution of impedance spectroscopy by using highly integrated silicon circuits to create a dense array of sensors, with the help of Chang's group [40]. We can use the silicon circuits to replace the network analyzer for generating and sensing the microwave signal as well as for on-chip signal processing to improve the signal-to-noise ratio. Because the impedance spectrum is made of broad relaxations, instead of sweeping across decades of frequency, the silicon circuits may need to work with only a few discrete frequencies, for example, 10 kHz for R_M, 10 MHz for C_M and R_C, and 10 GHz for C_C. Alternatively, a network analyzer can be built on a chip or board, following Kissinger's group [41].

For cytometer-like applications, we also need to improve the throughput. In microfluidics, we have used sheath flows to aim the cell-containing main flow at the trap on the CPW, which improves the throughput from about one cell/min to roughly 10 cells/min [34]. This is still a long way from the 100–1,000 cells/s of a typical cytometer. However, if we can show the promise of the technique, clever people will figure out ways to drastically improve its throughput and make a fortune from commercializing it. With their help, one day we may be able to buy a cheap little attachment for the smartphone and take it to a jungle to test for human immunodeficiency virus.

Acknowledgments

I thank the collaborators listed in the references, especially Y. Ning, X. Ma, X. Jin, and X. Du, who were my Ph.D. students at Lehigh University. I appreciate the discussion with R. Pethig, Edinburgh University. This work was supported, in part, by the U.S. Defense Threat Reduction Agency, under grant HDTRA1-12-1-0007; the U.S. Army Research Office, under grant W911NF-14-1-0665; the U.S. Air Force Office of Scientific Research, under grant FA9550-16-1-0475; and the U.S. National Science Foundation, under grant 1809623-ECCS.

References

[1] J. C. Maxwell, "Medium in which small spheres are uniformly disseminated," in *A Treatise on Electricity and Magnetisms*, 3rd ed. Oxford, U.K.: Clarendon Press, 1891, ch. 9, part 2, p. 440.

[2] K. W. Wagner, "Erklärung der dielektrischen nachwirkungsvorgange auf grund Maxwellscher vorstellungen," *Arch. Elektrotech.*, vol. 2, no. 9, pp. 371–387, Sept. 1914. doi: 10.1007/BF01657322.

[3] J. Bernstein, "Untersuchungen zur thermodynamik der bioelektrischen strome," *Arch. ges. Physiol.*, vol. 92, nos. 10–12, pp. 521–562, 1902. doi: 10.1007/BF01790181.

[4] X. Ma, X. Du, H. Li, X. Cheng, and J. C. M. Hwang, "Ultra-wideband impedance spectroscopy of a live biological cell," *IEEE Trans.*

Microw. Theory Techn., vol. 66, no. 8, pp. 3690–3696, Aug. 2018. doi: 10.1109/TMTT.2018.2851251.

[5] H. Li et al., "Distributed effect in high-frequency electroporation of biological cells," *IEEE Trans. Microw. Theory Techn.*, vol. 65, no. 9, pp. 3503–3511, Sept. 2017. doi: 10.1109/TMTT.2017.2659736.

[6] R. Höber, "Eine methode die elektrische leitfaehigkeit im innern von zellen zu messen," *Arch. ges. Physiol.*, vol. 133, nos. 4–6, pp. 237–259, 1910. [Online]. Available: https://hoebers.wordpress.com/2020/08/27/a-century-old-experiment-still-relevant-today/. doi: 10.1007/BF01680330.

[7] R. Pethig and I. Schmueser, "Marking 100 years since Rudolf Höber's discovery of the insulating envelope surrounding cells and of the β-dispersion exhibited by tissue," *J. Electr. Bioimp.*, vol. 3, no. 1, pp. 74–79, Nov. 2012. doi: 10.5617/jeb.401.

[8] A. Denzi et al., "Assessment of cytoplasm conductivity by nanosecond pulsed electric fields," *IEEE Trans. Biomed. Eng.*, vol. 62, no. 6, pp. 1595–1603, June 2015. doi: 10.1109/TBME.2015.2399250.

[9] Y. Ning et al., "Broadband electrical detection of individual biological cells," *IEEE Trans. Microw. Theory Techn.*, vol. 62, no. 9, pp. 1905–1911, Sept. 2014. doi: 10.1109/TMTT.2014.2342660.

[10] M. Philippson, "Les lois de la résistance électrique des tissus vivants," *Bull. Cl. Sci. Acad. R. Belg.*, vol. 7, no. 7, pp. 387–403, July 1921.

[11] H. Fricke, "The electric capacity of suspensions of a red corpuscles of a dog," *Phys. Rev.*, vol. 26, no. 5, pp. 682–687, Nov. 1925. doi: 10.1103/PhysRev.26.682.

[12] X. Ma, X. Du, L. Li, H. Li, X. Cheng, and J. C. M. Hwang, "Sensitivity analysis for ultra-wideband 2-port impedance spectroscopy of a live cell," *IEEE J. Electromagn. RF Microw. Med. Biol.*, vol. 4, no. 1, pp. 37–44, Mar. 2020. doi: 10.1109/JERM.2019.2921221.

[13] K. R. Foster, "Herman P. Schwan: A scientist and pioneer in biomedical engineering," *Annu. Rev. Biomed. Eng.*, vol. 4, no. 1, pp. 1–27, Aug. 2002. doi: 10.1146/annurev.bioeng.4.092001.093625.

[14] H. Hertz, *Electric Waves: Being Researches on the Propagation of Electric Action with Finite Velocity through Space*. Cambridge, U.K.: Dover, 1893.

[15] "Hugo Fricke Collection," CSHL Library and Collections. Cold Spring Harbor, New York: Cold Spring Harbor Laboratory, 2015. [Online]. Available: https://library.cshl.edu/personal-collections/hugo-fricke

[16] H. P. Schwan, "Electrical properties of tissue and cell suspensions," *Adv. Biol. Med. Phys.*, vol. 5, pp. 147–209, May 1957. doi: 10.1016/B978-1-4832-3111-2.50008-0.

[17] H. P. Schwan, "Analysis of dielectric data: Experience gained with biological materials," *IEEE Trans. Electr. Insul.*, vol. EI-20, no. 6, pp. 913–922, Dec. 1985. doi: 10.1109/TEI.1985.348727.

[18] F. Artis et al., "Microwaving biological cells: Intracellular analysis with microwave dielectric spectroscopy," *IEEE Microw. Mag.*, vol. 16, no. 4, pp. 87–96, May 2015. doi: 10.1109/MMM.2015.2393997.

[19] C. Merla, M. Liberti, F. Apollonio, and G. d'Inzeo, "Quantitative assessment of dielectric parameters for membrane lipid bi-layers from RF permittivity measurements," *Bioelectromagnetics*, vol. 30, no. 4, pp. 286–298, May 2009. doi: 10.1002/bem.20476.

[20] X. Du, X. Ma, H. Li, L. Li, X. Cheng, and J. C. M. Hwang, "Validation of Clausius-Mossotti function in wideband single-cell dielectrophoresis," *IEEE J. Electromagn. RF Microw. Med. Biol.*, vol. 3, no. 2, pp. 127–133, June 2019. doi: 10.1109/JERM.2019.2894100.

[21] H. Li, X. Ma, X. Du, L. Li, X. Cheng, and J. C. M. Hwang, "Correlation between optical fluorescence and microwave transmission during single-cell electroporation," *IEEE Trans. Biomed. Eng.*, vol. 66, no. 8, pp. 2223–2230, Aug. 2019. doi: 10.1109/TBME.2018.2885781.

[22] X. Ma, X. Du, L. Li, C. Ladegard, X. Cheng, and J. C. M. Hwang, "Broadband electrical characterization of a live biological cell with in situ single-connection calibration," *Sensors*, vol. 20, no. 14, p. 3844, July 2020. doi: 10.3390/s20143844.

[23] H. P. Schwan, "Electrode polarization impedance and measurements in biological materials," *Ann. New York Acad. Sci.*, vol. 148, no. 1, pp. 191–209, Feb. 1968. doi: 10.1111/j.1749-6632.1968.tb20349.x.

[24] X. Ma et al., "Reproducible broadband measurement for cytoplasm capacitance of a biological cell," in *Proc. IEEE MTT-S Int. Microw. Symp. (IMS)*, May 2016, pp. 1–4. doi: 10.1109/MWSYM.2016.7540262.

[25] R. T. Abraham and A. Weiss, "Jurkat T cells and development of the T-cell receptor signaling paradigm," *Nat. Rev. Immunol.*, vol. 4, no. 4, pp. 301–308, Apr. 2004. doi: 10.1038/nri1330.

[26] F. F. Becker, X. B. Wang, Y. Huang, R. Pethig, J. Vykoukal, and P. R. Gascoyne, "Separation of human breast cancer cells from blood by differential dielectric affinity," *Proc. Nat. Acad. Sci. USA*, vol. 92, no. 3, pp. 860–864, Jan. 1995. doi: 10.1073/pnas.92.3.860.

[27] I. Ermolina, Y. Polevaya, Y. Feldman, B. Z. Ginzburg, and M. Schlesinger, "Study of normal and malignant white blood cells by time domain dielectric spectroscopy," *IEEE Trans. Dielectr. Electr. Insul.*, vol. 8, no. 2, pp. 253–261, Apr. 2001. doi: 10.1109/94.919948.

[28] M. Kiesel et al., "Swelling-activated pathways in human T-lymphocytes studied by cell volumetry and electrorotation," *Biophys. J.*, vol. 90, no. 12, pp. 4720–4729, Feb. 2006. doi: 10.1529/biophysj.105.078725.

[29] A. L. Garner et al., "Ultrashort electric pulse induced changes in cellular dielectric properties," *Biochem. Biophys. Res. Commun.*, vol. 362, no. 1, pp. 139–144, Oct. 2007. doi: 10.1016/j.bbrc.2007.07.159.

[30] A. C. Sabuncu, J. Zhuang, J. F. Kolb, and A. Beskok, "Microfluidic impedance spectroscopy as a tool for quantitative biology and biotechnology," *Biomicofluidics*, vol. 6, no. 3, p. 034103, June 2012. doi: 10.1063/1.4737121.

[31] S. I. Han, Y. D. Joo, and K. H. Han, "An electrorotation technique for measuring the dielectric properties of cells with simultaneous use of negative quadrupolar dielectrophoresis and electrorotation," *Analyst*, vol. 138, no. 5, pp. 1529–1537, Jan. 2013. doi: 10.1039/c3an36261b.

[32] K. Asami, Y. Takahashi, and S. Tabshima, "Dielectric properties of mouse lymphocytes and erythrocytes," *Biochim. Biophys. Acta*, vol. 1010, no. 1, pp. 49–55, Jan. 1989. doi: 10.1016/0167-4889(89)90183-3.

[33] A. Denzi et al., "Microdosimetric study for nanosecond pulsed electric fields on a cell circuit model with nucleus," *J. Membr. Biol.*, vol. 246, no. 10, pp. 761–767, Oct. 2013. doi: 10.1007/s00232-013-9546-7.

[34] X. Du, C. Ladegard, X. Ma, X. Cheng, and J. C. M. Hwang, "Broadband electrical sensing of nucleus size in a live cell from 900 Hz to 40 GHz," in *Proc. IEEE Int. Conf. Biomed. Appl. (IMBioC)*, Dec. 2020, pp. 1–3.

[35] X. Ma et al., "A multistate single-connection calibration for microwave-microfluidics," *IEEE Trans. Microw. Theory Techn.*, vol. 66, no. 2, pp. 1099–1107, Feb. 2018. doi: 10.1109/TMTT.2017.2758364.

[36] J. C. Chien, A. Ameri, E.-C. Yeh, A. N. Killilea, M. Anwar, and A. M. Niknejad, "A high-throughput flow cytometry-on-a-CMOS platform for single-cell dielectric spectroscopy at microwave frequencies," *Lab Chip*, vol. 18, no. 14, pp. 2065–2076, May 2018. doi: 10.1039/C8LC00299A.

[37] X. Jin, M. Farina, X. Wang, G. Fabi, X. Cheng, and J. C. M. Hwang, "Quantitative scanning microwave microscopy of the evolution of a live biological cell in a physiological buffer," *IEEE Trans. Microw. Theory Techn.*, vol. 67, no. 12, pp. 5438–5445, Dec. 2019. doi: 10.1109/TMTT.2019.2941850.

[38] M. Farina and J. C. M. Hwang, "Scanning microwave microscopy for biological applications: Introducing the state of the art and inverted SMM," *IEEE Microw. Mag.*, vol. 21, no. 10, pp. 52–59, Oct. 2020. doi: 10.1109/MMM.2020.3008239.

[39] H. Li et al., "Differentiation of live and heat-killed E. coli by microwave impedance spectroscopy," *Sens. Actuators B*, vol. 255, no. 2, pp. 1614–1622, Feb. 2018. doi: 10.1016/j.snb.2017.08.179.

[40] J. Zhou et al., "A silicon-based closed-loop 256-Pixel near-field capacitive sensing array with 3-ppm sensitivity and selectable frequency shift gain," in *Proc. IEEE MTT-S Int. Microw. Symp. (IMS)*, Aug. 2020, pp. 464–467. doi: 10.1109/IMS30576.2020.9224059.

[41] D. Wang et al., "Integrated 240-GHz dielectric sensor with DC readout circuit in a 130-nm SiGe BiCMOS technology," *IEEE Trans. Microw. Theory Techn.*, vol. 66, no. 9, pp. 4232–4241, Sept. 2018. doi: 10.1109/TMTT.2018.2839104.